Electronic Supplementary Material (ESI) for New Journal of Chemistry.

Naked-eye colorimetric sensor for methanol and 'turn-on' fluorescence detection of Al^{3+}

Virendra Kumar,* Subhankar Kundu, Bahadur Sk and Abhijit Patra

Indian Institute of Science Education and Research Bhopal, Indore Bypass Road, Bhauri, Bhopal 462066, Madhya Pradesh India

1. Characterization of NRSB and NRSB-O

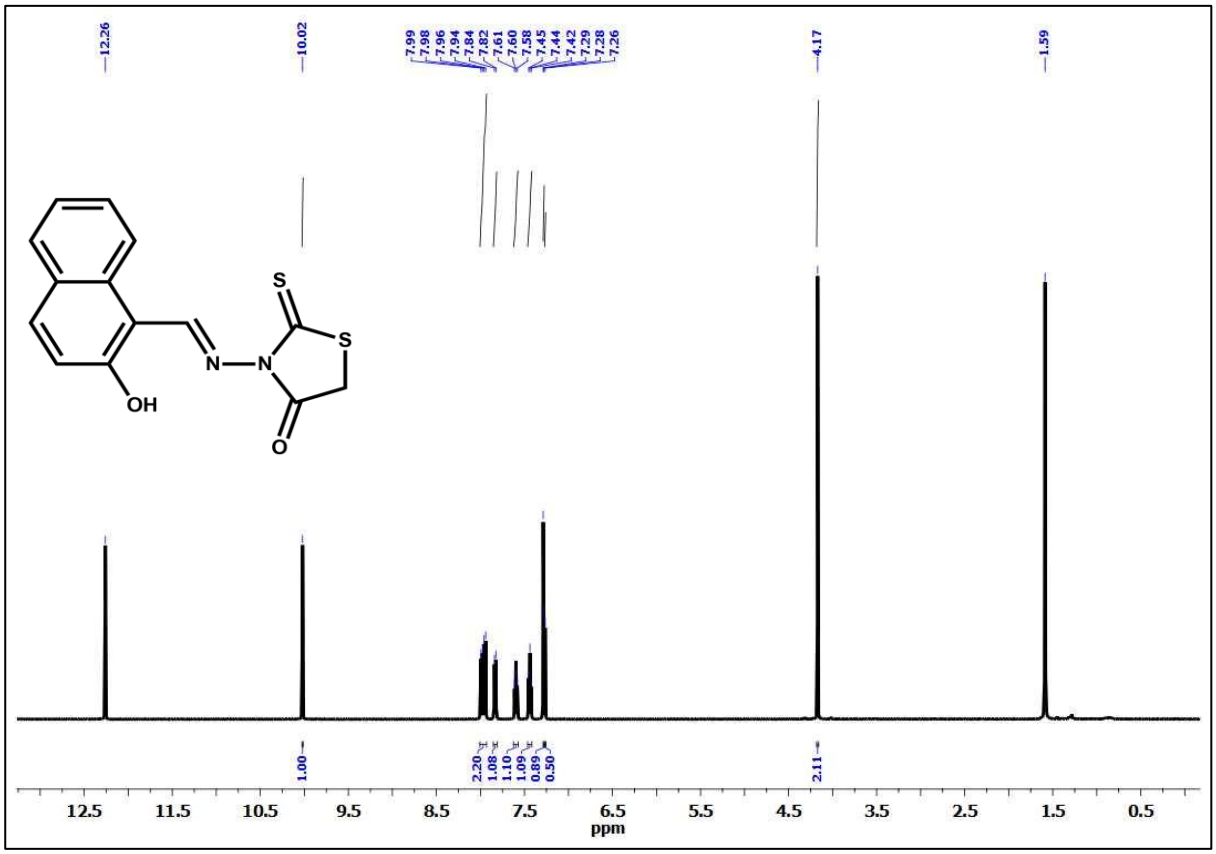

Fig. S1 ^{1}H NMR spectrum of NRSB in $CDCl_3$ at room temperature.

^{1}H NMR (500 MHz, CDCl3): δ 12.26 (s, 1H), 10.02 (s, 1H), 7.97 (dd, J = 18.4, 8.8 Hz, 2H), 7.83 (d, J = 8.0 Hz, 1H), 7.62 – 7.57 (m, 1H), 7.44 (t, J = 7.1 Hz, 1H), 7.28 (d, J = 2.3 Hz, 1H), 7.26 (s, 1H), 4.17 (s, 2H).

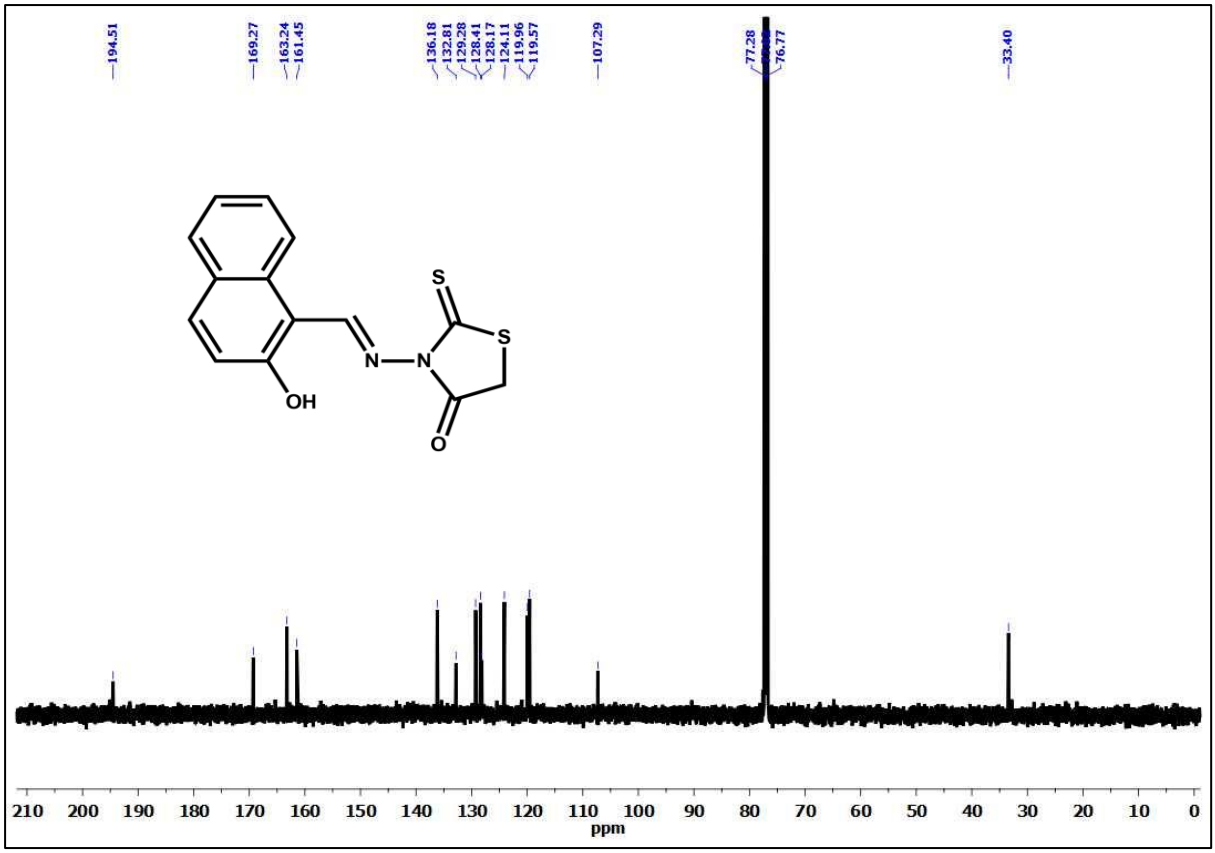

Fig. S2 ^{13}C NMR spectrum of NRSB in $CDCl_3$ at room temperature.

^{13}C NMR (126 MHz, $CDCl_3$): δ 194.51, 169.27, 163.24, 161.45, 136.18, 132.81, 129.28, 128.41, 128.17, 124.11, 119.96, 119.57, 107.29, 77.28, 77.02, 76.77, 33.40.

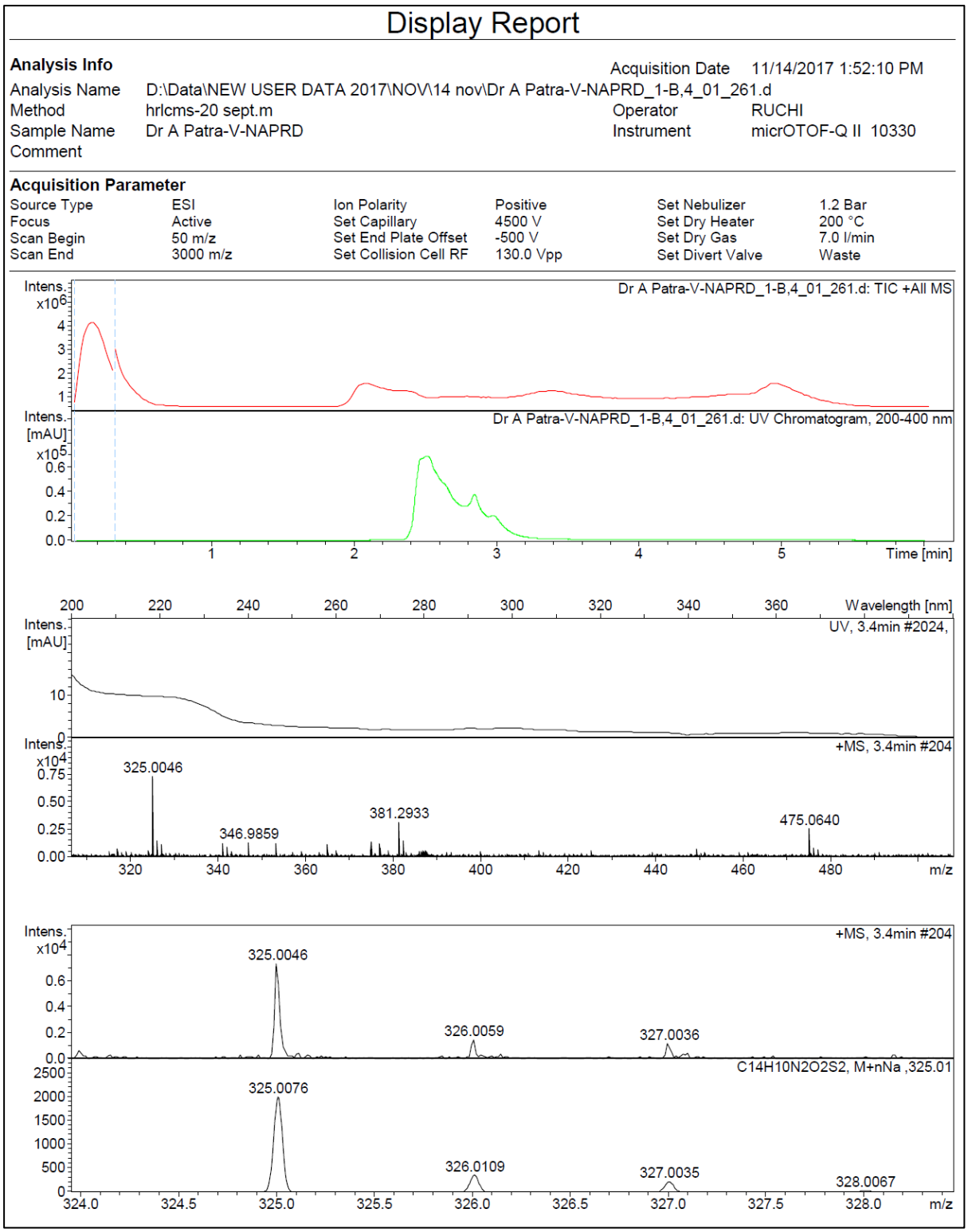

Fig. S3 HRMS spectrum of NRSB.

HRMS: m/z calculated $C_{14}H_{10}N_2O_2S_2Na$ Exact Mass: 325.0076 Found $[M]^+$: 325.0046.

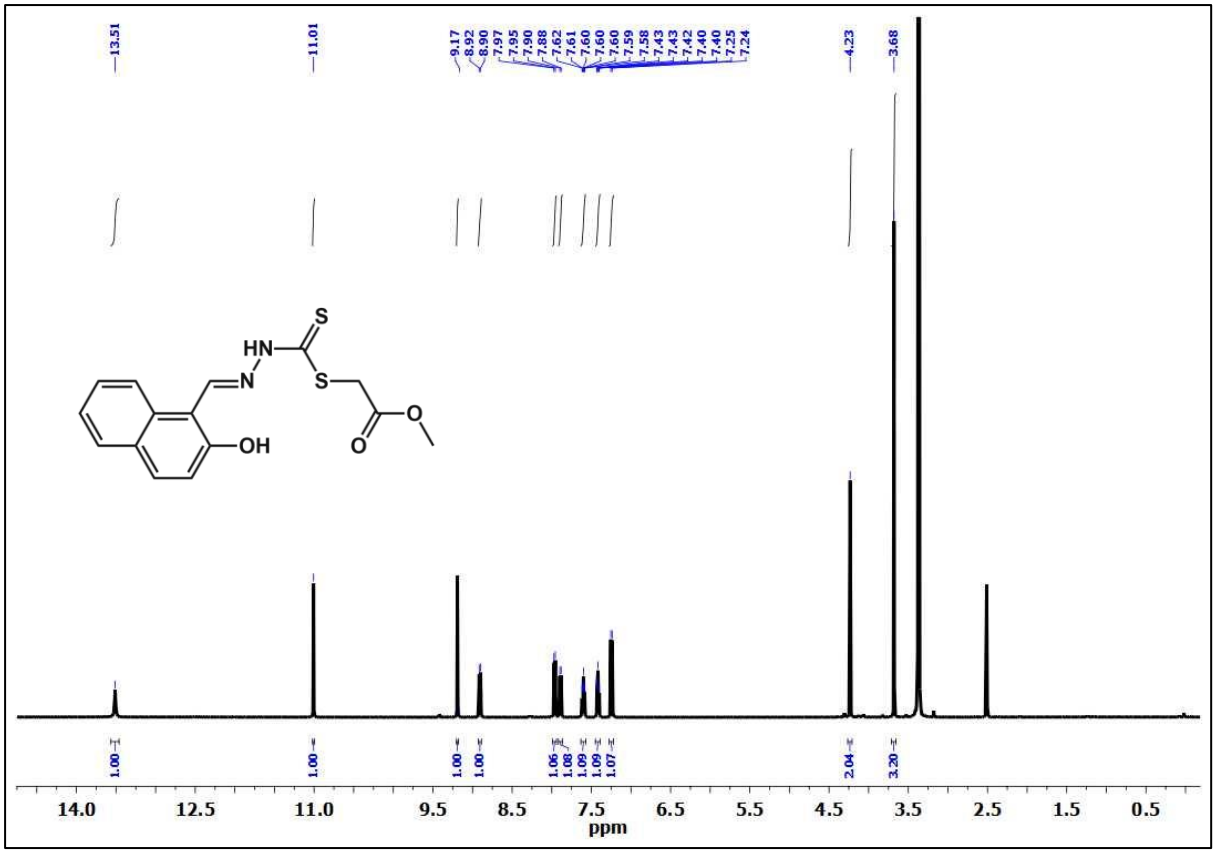

Fig. S4 ^{1}H NMR spectrum of NRSB-O in DMSO-d_6 at room temperature.

^{1}H NMR (500 MHz, DMSO-d_6): δ 13.51 (s, 1H), 11.01 (s, 1H), 9.19 (s, 1H), 8.91 (d, J = 8.6 Hz, 1H), 7.96 (d, J = 8.9 Hz, 1H), 7.89 (d, J = 7.9 Hz, 1H), 7.60 (dd, J = 8.4, 6.9, 1.3 Hz, 1H), 7.45 – 7.39 (m, 1H), 7.25 (d, J = 8.9 Hz, 1H), 4.23 (s, 2H), 3.68 (s, 3H).

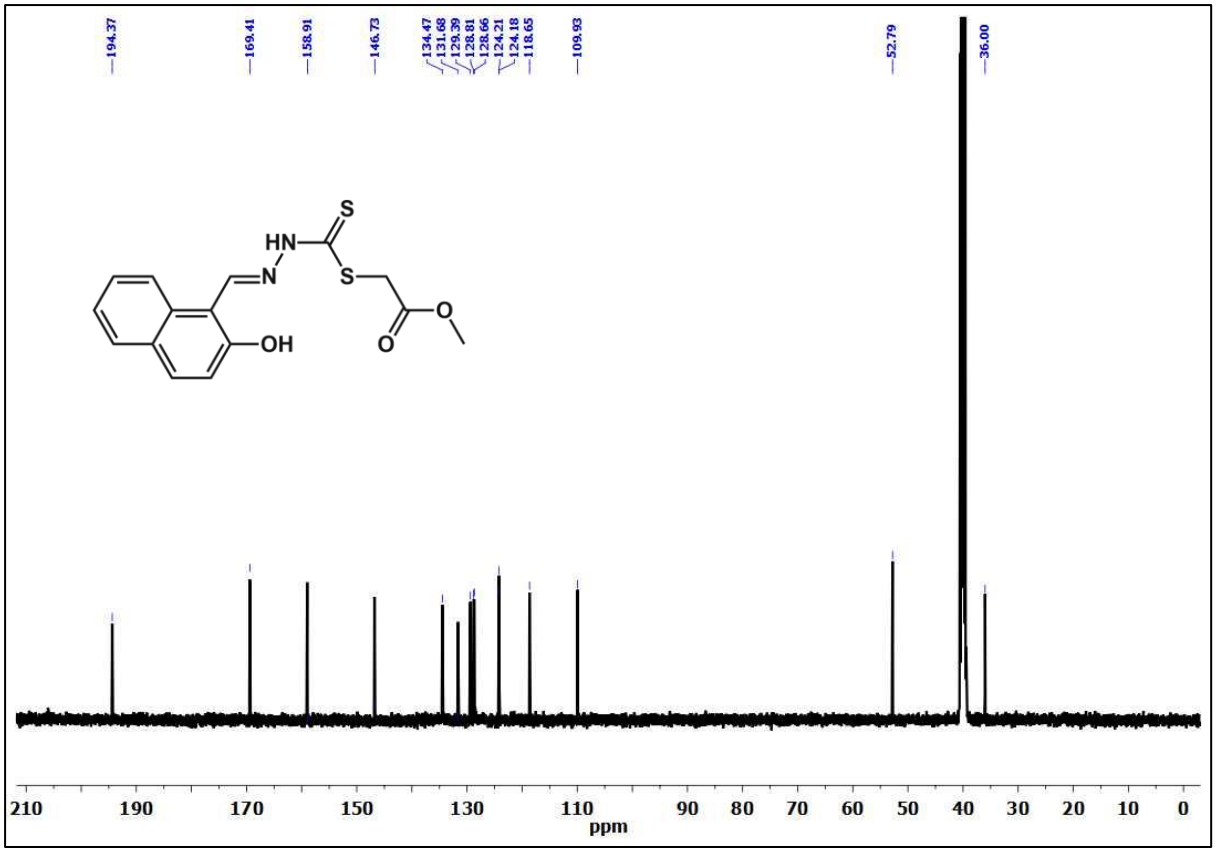

Fig. S5 ^{13}C NMR spectrum of NRSB-O in DMSO-d_6 at room temperature.

^{13}C NMR (126 MHz, DMSO-d_6): δ 194.37, 169.41, 158.91, 146.73, 134.47, 131.68, 129.39, 128.81, 128.66, 124.21, 124.18, 118.65, 109.93, 52.79, 36.00.

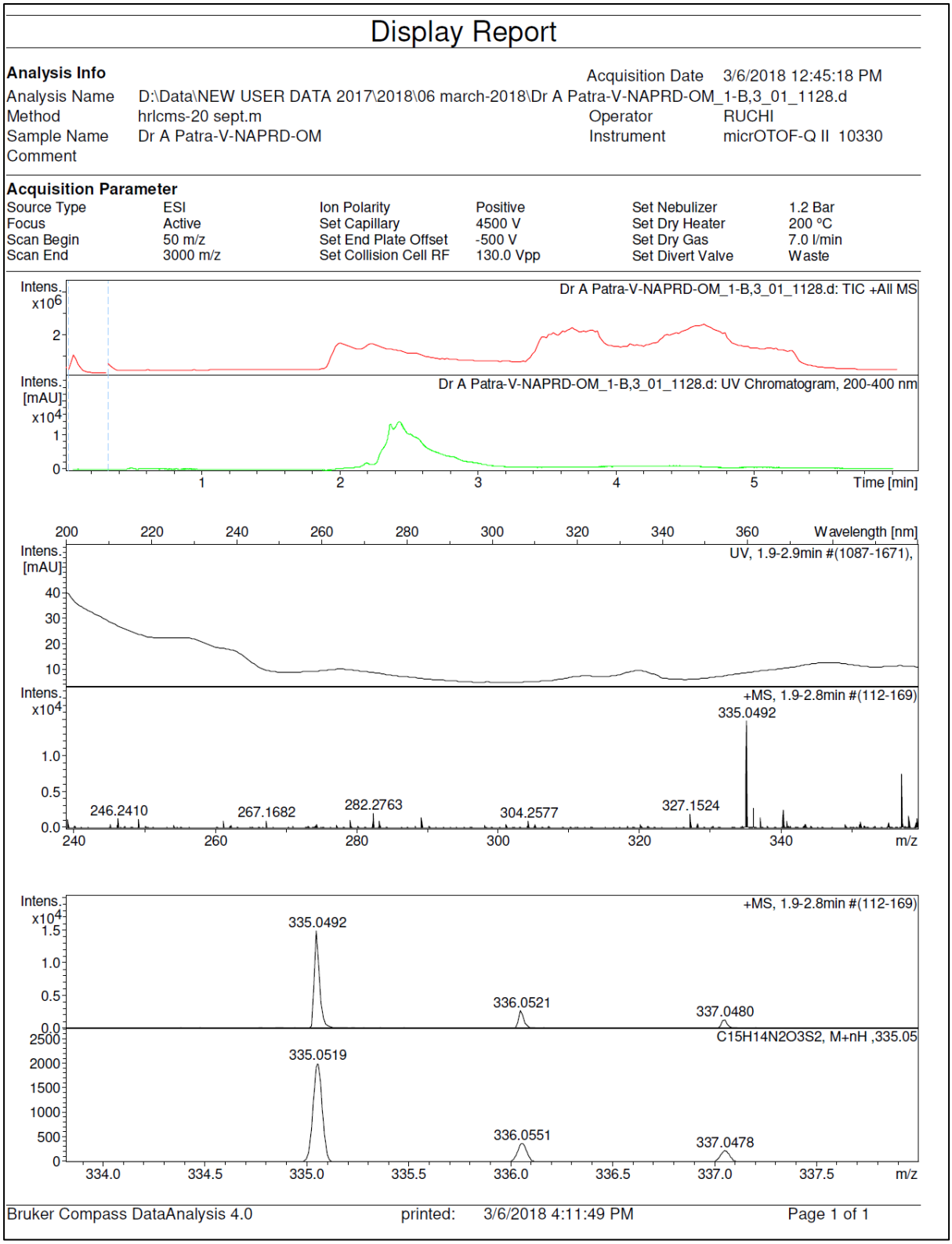

Fig. S6 HRMS spectrum of NRSB-O.

HRMS: m/z Calculated $C_{15}H_{14}N_2O_3S_2$, Exact Mass: 334.0446 Found $[M+H]^+$: 335.0492.

Table S1. Crystal data and structure refinement for NRSB.

Identification code	NRSB (CCDC 1914399)
Empirical formula	$C_{14}H_{10}N_2O_2S_2$
Formula weight	302.36
Temperature	296 (2) K
Wavelength	0.71073 Å
Crystal system, space group	Monoclinic, $P2_{1/n}$
Unit cell dimensions	a = 18.3344(6) Å alpha = 90 deg. b = 7.2653(3) Å beta = 106.564(2) deg. c = 30.4160(10) Å gamma = 90 deg.
Volume	3883.4(2) $Å^3$
Z, Calculated density	12, 1.551 mg/m^3
Absorption coefficient	0.413 mm^{-1}
F(000)	1872.0
Theta range for data collection	3.133 to 27.103 deg.
Limiting indices	-23<=h<=23, -9<=k<=9, -38<=l<=38
Reflections collected / unique	28386 / 8524 [R(int) = 0.0863]
Completeness to theta = 25.000	99.4 %
Absorption correction	None
Refinement method	Full-matrix least-squares on F^2
Data / restraints / parameters	8524 / 0 / 661
Goodness-of-fit on F^2	1.030
Final R indices [I>2sigma(I)]	R1 = 0.0527, wR2 = 0.1132
R indices (all data)	R1 = 0.0899, wR2 = 0.1294
Largest diff. peak and hole	0.363 and -0.418 $e.A^{-3}$

Table S2. Crystal data and structure refinement for NRSB-O.

Identification code	NRSB-O (CCDC 1914400)
Empirical formula	$C_{15}H_{14}N_2O_3S_2$
Formula weight	334.40
Temperature	100(2) K
Wavelength	0.71073 Å
Crystal system, space group	Monoclinic, $P2_{1/c}$
Unit cell dimensions	a = 12.9330(6) Å α = 90 deg. b = 8.4524(4) Å β = 114.537(2) deg. c = 14.8255(7) Å γ = 90 deg.
Volume	1474.29(12) $Å^3$
Z, Calculated density	4, 1.507 mg/m^3
Absorption coefficient	0.375 mm^{-1}
F(000)	696.0
Theta range for data collection	2.789 to 30.525 deg.
Limiting indices	-18<=h<=18, -12<=k<=12, -17<=l<=21
Reflections collected / unique	21523 / 4489 [R(int) = 0.0856]
Completeness to theta = 25.000	99.9 %
Absorption correction	None
Refinement method	Full-matrix least-squares on F^2
Data / restraints / parameters	4489 / 0 / 255
Goodness-of-fit on F^2	1.033
Final R indices [I>2sigma(I)]	R1 = 0.0534, wR2 = 0.0937
R indices (all data)	R1 = 0.0965, wR2 = 0.1080
Largest diff. peak and hole	0.488 and -0.460 $e.A^{-3}$

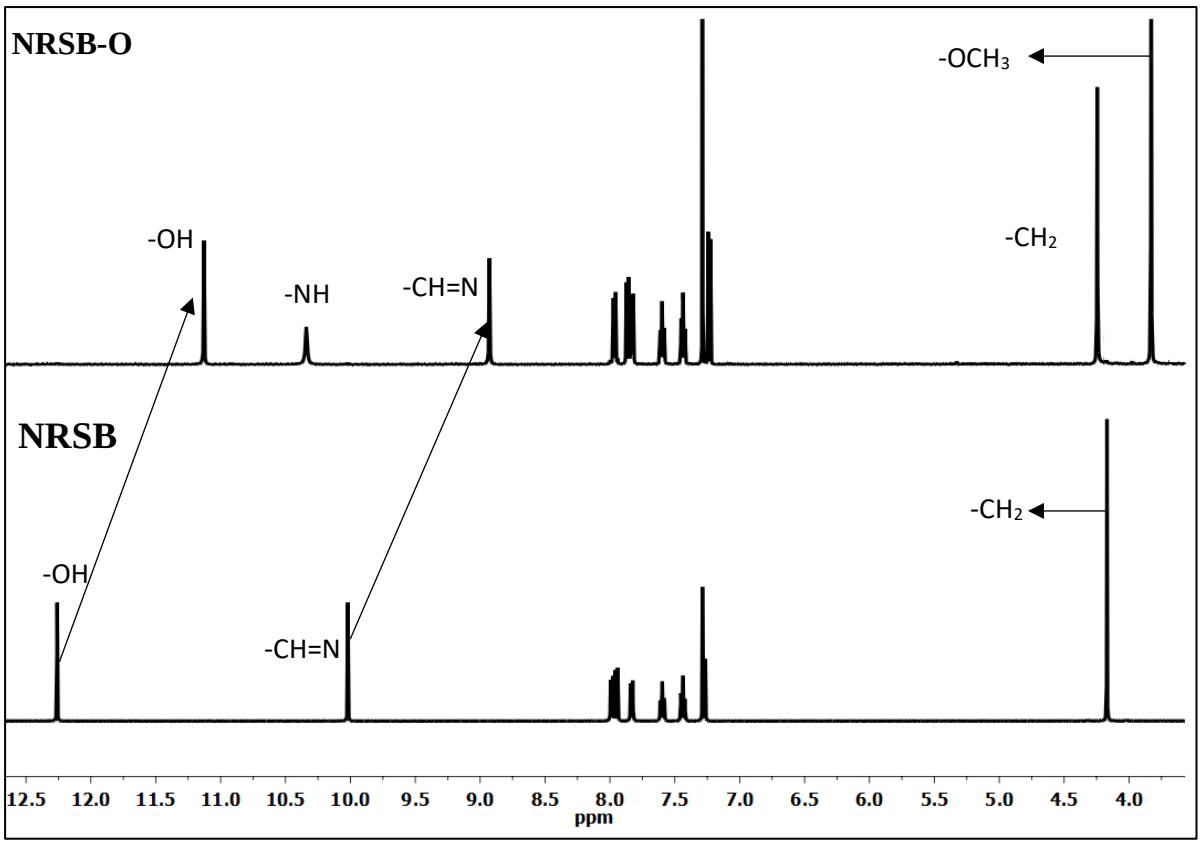

Fig. S7 ^{1}H NMR spectra of NRSB and NRSB-O in $CDCl_3$ (solid obtained by MeOH treatment of NRSB followed by solvent evaporation and drying).

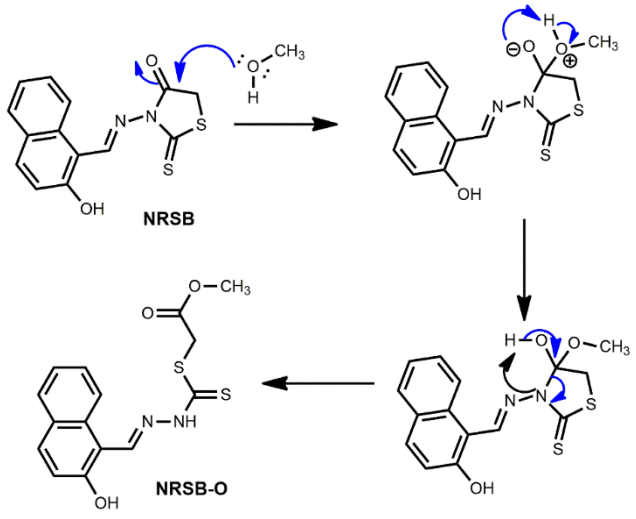

Fig. S8 Plausible ring opening mechanism for the conversion of NRSB to NRSB-O through the nucleophilic attack of methanol.

2. Methanol sensing study

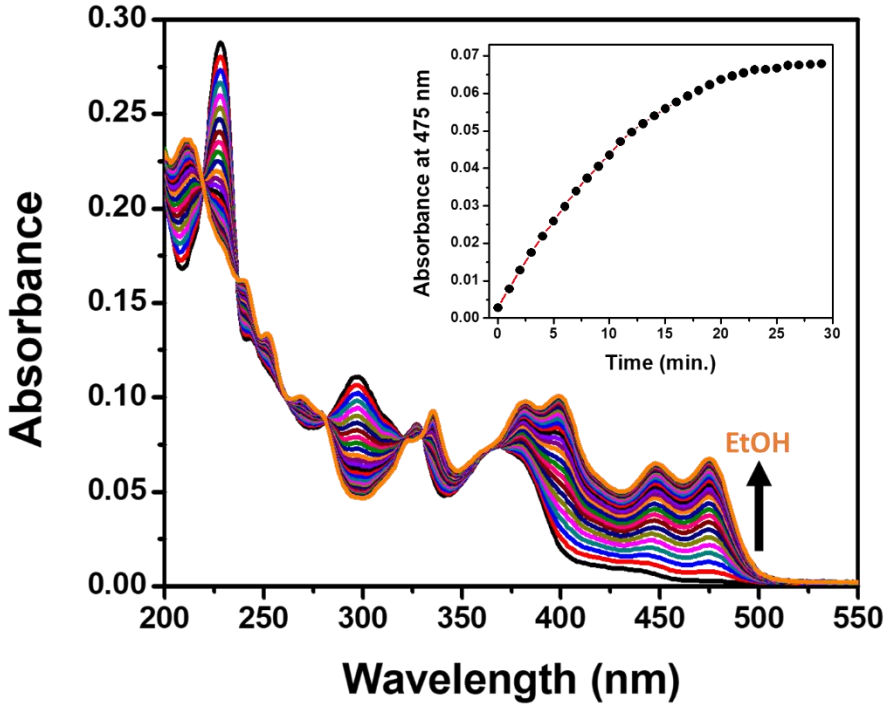

Fig. S9 Time-dependent absorption spectra of NRSB (5 μM) in absolute ethanol; absorbance at 475 nm vs. time plot (inset).

Calculation of limit of detection:

The limit of detection (LOD) was calculated by the following equations.[1] LOD = 3σ/S where σ is the standard deviation of the blank sample and S is the slope of the calibration curve, respectively. The limit of detection of methanol by NRSB in acetonitrile was determined using absorption spectroscopy. The calibration curve of NRSB was obtained by plotting the absorbance at 470 nm against the fraction of methanol (Fig. S10). The slope S was obtained from the above curve. The detection limit of NRSB was found to be 0.43 wt%.

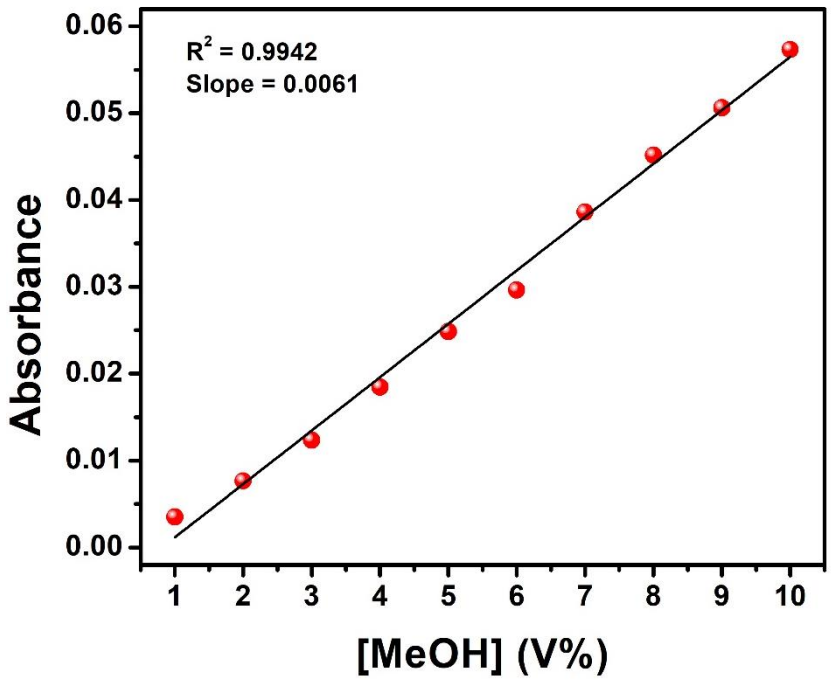

Fig. S10 Calibration curve of NRSB (5 μM) in acetonitrile with increasing fraction of methanol.

Crystal structure of NRSB and NRSB-O:

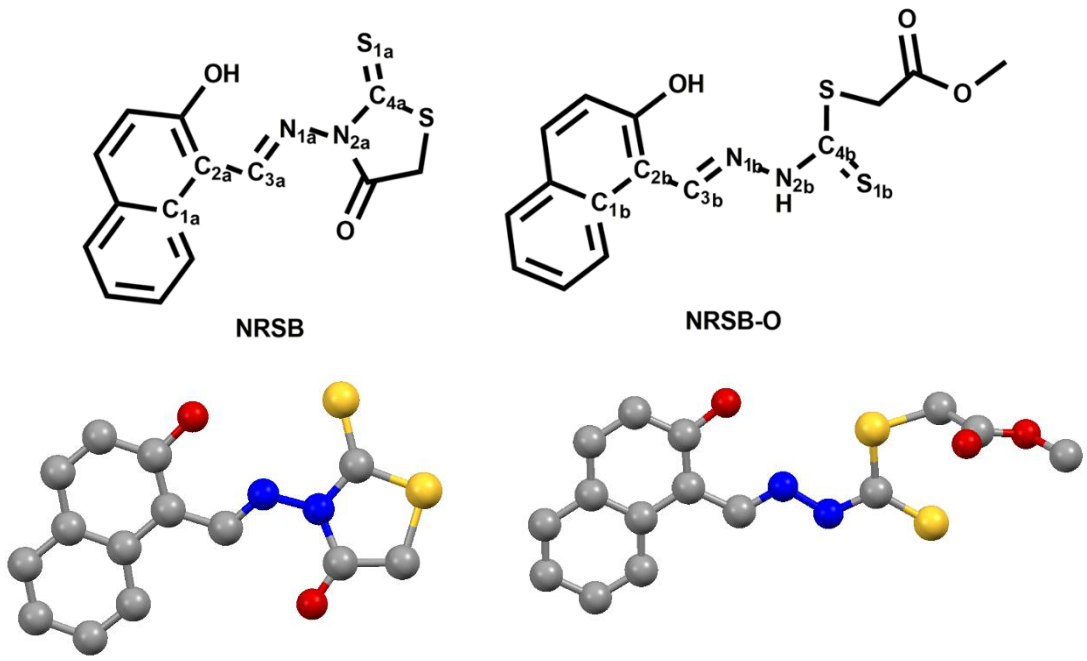

Crystal packing of NRSB and NRSB-O:

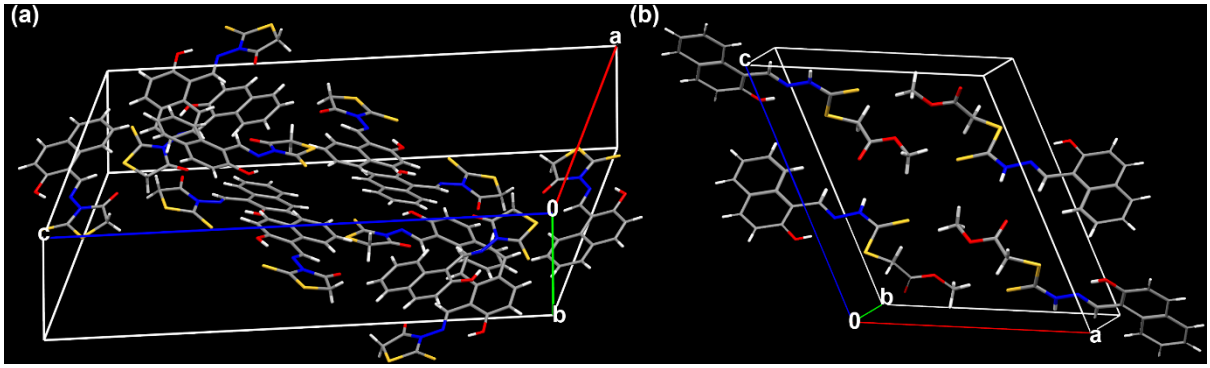

Fig. S11 The unit cell packing of (a) NRSB and (b) NRSB-O, obtained through the crystal structure analysis.

Table S3: The selected experimental and calculated dihedral angles in NRSB and NRSB-O.

Dihedral angles of NRSB and NRSB-O

DA1 = C1a-C2a-C3a-N1a DA11 = C1b-C2b-C3b-N1b

DA2= C2a-C3a-N1a-N2a DA22 = C2b-C3b-N1b-N2b

DA3 = C3a-N1a-N2a-C4a DA33 = C3b-N1b-N2b-C4b

DA4 = N1a-N2a-C4a-S1a DA44 = N1b-N2b-C4b-S1b

Dihedral angles from the DFT-optimized structure							
NRSB				NRSB-O			
DA1	DA2	DA3	DA4	DA11	DA22	DA33	DA44
-173.68	-179.28	147.46	-8.68	-179.85	-179.96	-179.85	-179.52
Dihedral angles from single crystal X-ray diffraction analysis							
NRSB				NRSB-O			
DA1	DA2	DA3	DA4	DA11	DA22	DA33	DA44
-177.35	-177.74	161.21	-4.46	-175.76	-179.69	-178.98	-178.85

Table S4: A comparative table of NRSB for optical detection and discrimination of methanol with some notable small organic molecules.

S. No.	Systems	Optical detection of Methanol		Selective discrimination of methanol in mixture of solvent	Limit of detection (LOD) of MeOH (wt%)		[Ref.]
		Colorimetric method	Fluorometric method		Colorimetric method	Fluorometric method	
1.	NRSB	Yes	No	Yes	0.43	-	Present work
2.	ZR1	Yes	Yes	Yes	-	0.038	[2]
3.	TTO	No	Yes	Yes	-	0.97	[3]
4.	DBAB	No	Yes	No	-	-	[4]
5.	DPP	No	Yes	No	-	-	[5]
6.	RC	No	Yes	Yes	-	0.042	[6]
7.	1, 2, 3	Yes	No	No	-	-	[7]
8.	OXP	Yes	No	Yes	-	-	[8]
9.	SPC	Yes	No	Yes	-	-	[9]
10.	NO_2-H_2SALNN	No	Yes	Yes	-	-	[10]
11.	HOF	No	Yes	Yes	-	-	[11]

3. Detection of Al^{3+}

The recognition of metal ions by NRSB-O was carried out through UV-Visible absorption and fluorescence spectroscopic analysis. The absorption spectra of NRSB-O (5 µM) was recorded in MeOH : H_2O (8 : 2) solvent mixture. It exhibited strong absorption at 470, 445 and 385 nm. The UV-Visible absorption study revealed that NRSB-O was non-selective towards the metal ions (Na^+, K^+, Mg^{2+}, Ca^{2+}, Mn^{2+}, Co^{2+}, Ni^{2+}, Cu^{2+}, Zn^{2+}, Cd^{2+}, Hg^{2+}, Pb^{2+}, Fe^{3+}, Al^{3+}, and Cr^{3+}, Fig. S12). We checked the fluorescence emission spectra of NRSB-O in the absence and the presence of different metal ions (λ_{ex} = 310 nm) in semi-aqueous solution MeOH : H_2O (8 : 2, v/v). A strong turn-on fluorescence response was observed in the presence of Al^{3+} ion only (Fig. S13).

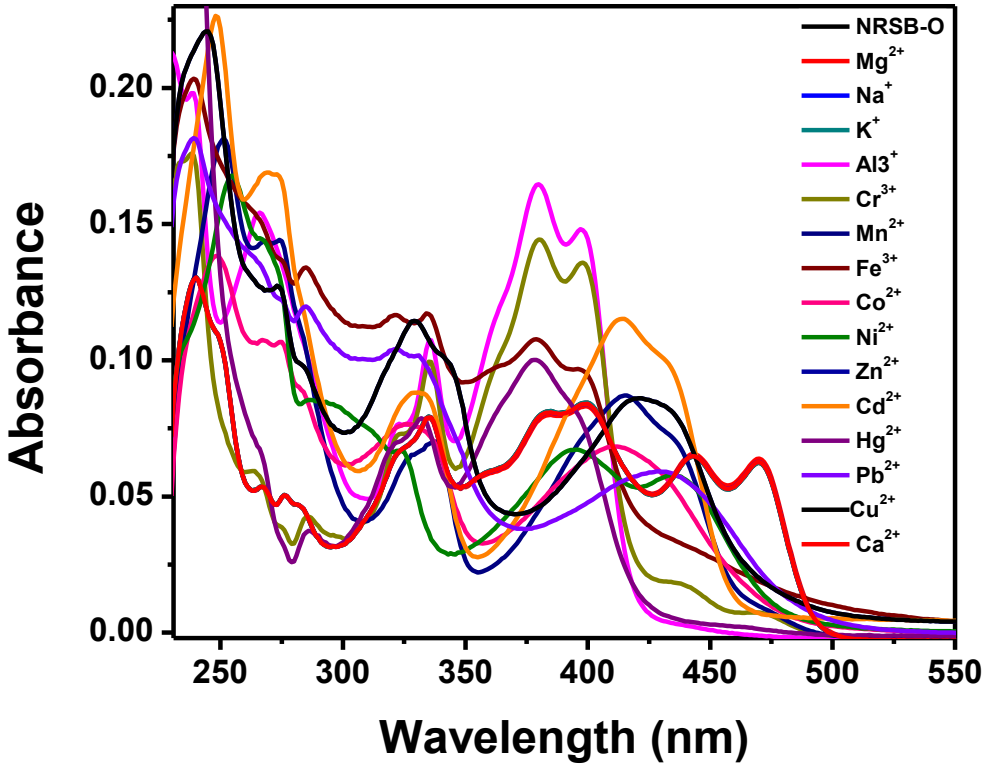

Fig. S12 Absorption spectra of NRSB-O (5 µM) with different metal ions (10 equiv.) in MeOH : H_2O (8 : 2, v/v) mixture solvent.

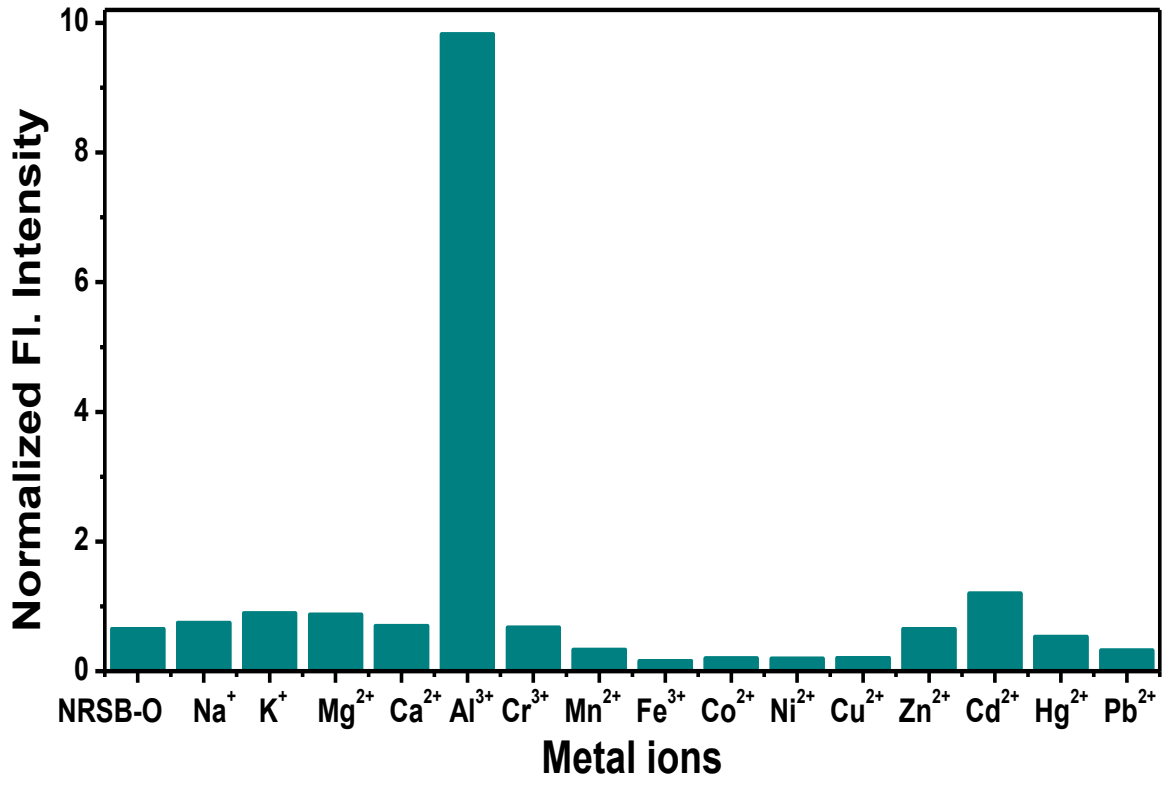

Fig. S13 Bar diagram of normalized fluorescence intensity of NRSB-O (5 μM) with different metal ions in MeOH : H_2O (8 : 2, v/v) solvent mixture.

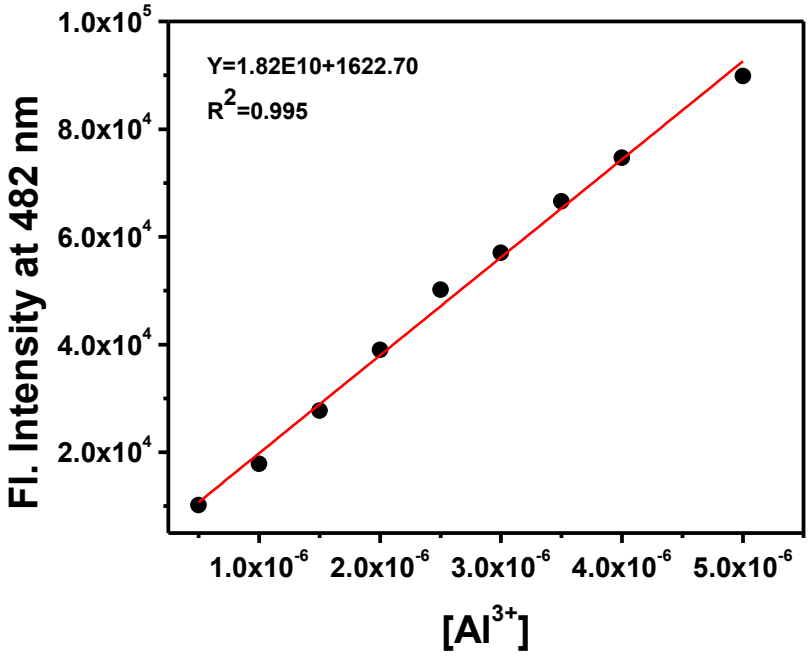

Fig. S14 Determination of the lowest detection limit (LOD) and the calibration curve of NRSB-O with Al^{3+}.

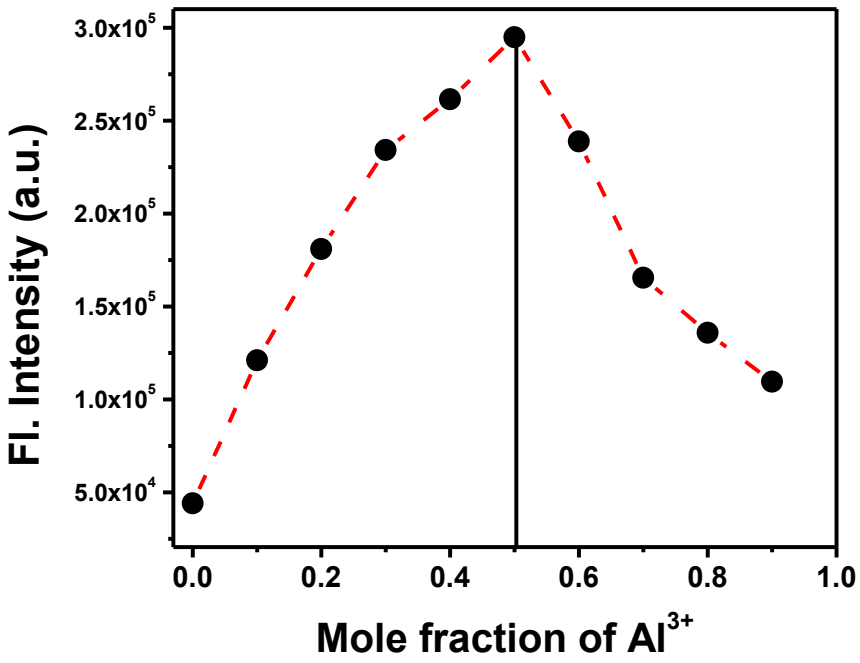

Fig. S15 Job's plot for NRSB-O and Al^{3+}. The fluorescence intensity at 480 nm was plotted against the mole fraction of aluminium ions. The total concentration of NRSB-O and Al^{3+} is 50 µM.

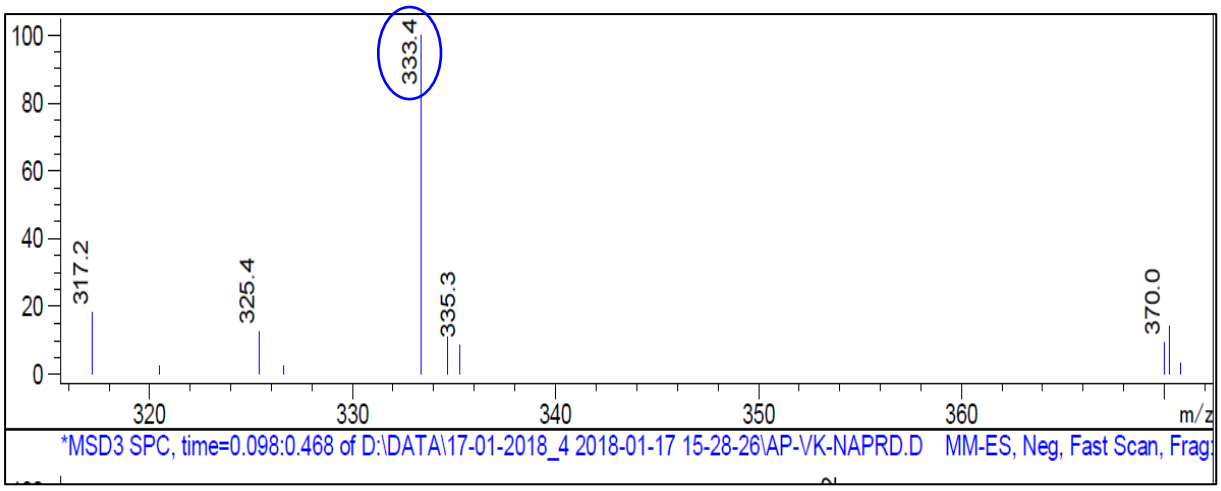

Fig. S16 LC-MS spectrum of NRSB-O.

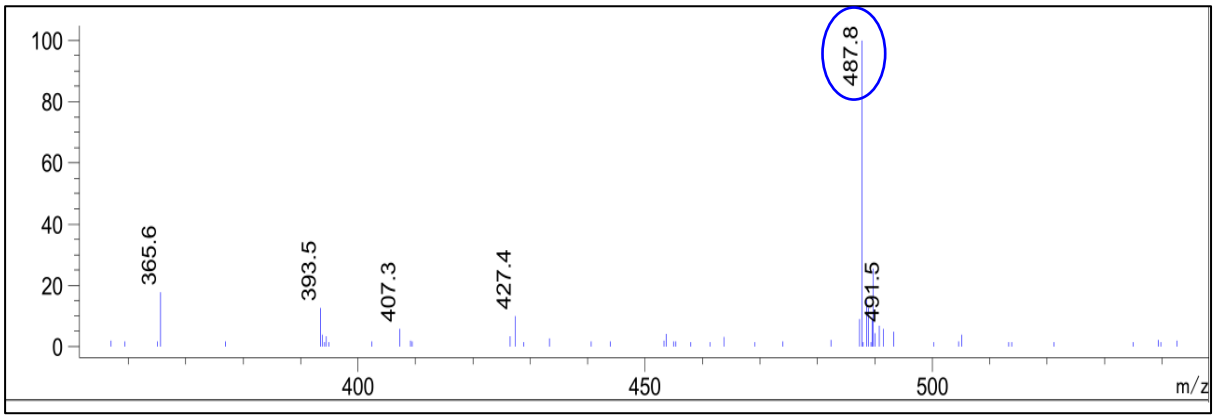

Fig. S17 LC-MS spectrum of NRSB-O with Al^{3+}.

Calculation of association constant:

The binding constants (K) was obtained by a non-linear least squares analysis of F versus C_0 and Cm using the following 1:1 binding equation.[12]

$$F = F_0 + \frac{F_{lim} - F}{2C_0}\left[C_0 + C_m + \frac{1}{K} - \sqrt{\left\{\left(C_0 + C_m + \frac{1}{K}\right)^2 - 4C_m C_0\right\}}\right] \quad ----(1)$$

Where, F: fluorescence intensity of the solution in presence of Al^{3+} during the titration; F_0: fluorescence intensity of NRSB-O in the absence of Al^{3+}; F_{lim}: fluorescence intensity of NRSB-O and Al^{3+} upon saturation; C_0: concentration of NRSB-O; C_m: concentration of Al^{3+} during the course of titration; and K: equilibrium constant of the complex. The sigmoidal curve was obtained by plotting the fluorescence intensity of NRSB-O at 482 nm against increasing concentration of Al^{3+}. The association constant of NRSB-O for Al^{3+} was found to be 2.85×10^5 (Correlation coefficient, $R^2 = 0.993$, Fig. S18).

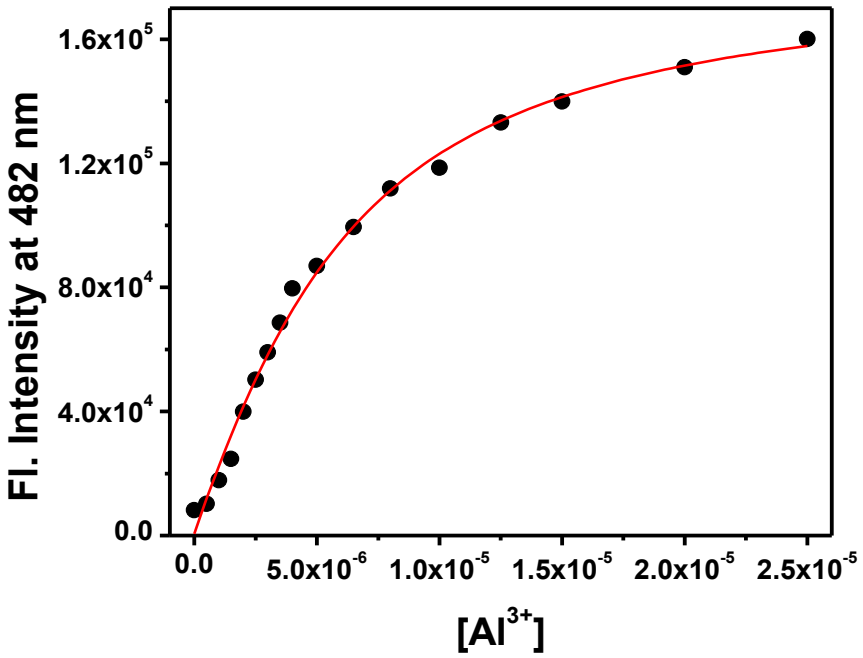

Fig. S18 Binding constant determination of NRSB-O with Al^{3+} form non-linear least squares fitting of fluorescence data.

Proposed complex of NRSB-O and Al^{3+}:

In general, Al^{3+} can bind with the ligands through (i) three coordination or (ii) by six coordination modes.[14,15] No complexation occurs between NRSB (close form) and Al^{3+}. The highly constrained structure and the presence of two quaternary nitrogen centres may prevent the complexation (Scheme S1). On the other hand, the flexible NRSB-O (open form) in the presence of Al^{3+} led to the formation of the stable NRSB-O-Al^{3+} complex presumably through six coordination mode. We could not get the crystal of the complex even after multiple attempts. But the nature of the coordination of NRSB-O with Al^{3+} ion was examined through Job's plot (fluorescence method) and mass spectrometry analysis. The Job's plot indicated the 1:1 complexation between NRSB-O and Al^{3+} (Fig. S15) and the mass analysis confirmed the presence of two chlorine (Cl) atoms and one -OCH_3 group in the coordination complex (Fig. S17).

^1H NMR spectroscopy was also used to elucidate the binding mode of **NRSB-O** to Al^{3+}. ^1H NMR spectra of **NRSB-O** were recorded in DMSO-d_6 with increasing concentrations of Al^{3+} (as its chloride salt solution in D_2O). On addition of Al^{3+} (0 to 5 equiv.) to the **NRSB-O**, significant spectral changes were observed (Fig. S19). The peak due to phenolic proton (H1) at 13.50 ppm progressively disappear, suggesting the deprotonation during the coordination to metal ions. However, binding to the electron deficient Al^{3+} strengthen the electron-withdrawing ability of the imine nitrogen of NRSB-O. As a consequence, the adjacent NH proton resonates from 11 ppm to 11.2 ppm due to the decrease of electron density. The aldimine proton peak of NRSB-O (9.20 ppm) shows a slight upfield shift (9.14 ppm) which clearly supports the coordination of the aldimine nitrogen with Al^{3+}. Additionally, the signals for the aromatic protons are also shifted compared to that of the spectrum of free NRSB-O. Thus, on the basis of Job's plot, mass spectrometry analysis and the ^1H NMR studies, the most probable structure of the complex is proposed in Scheme S1 and Scheme 2, main text.

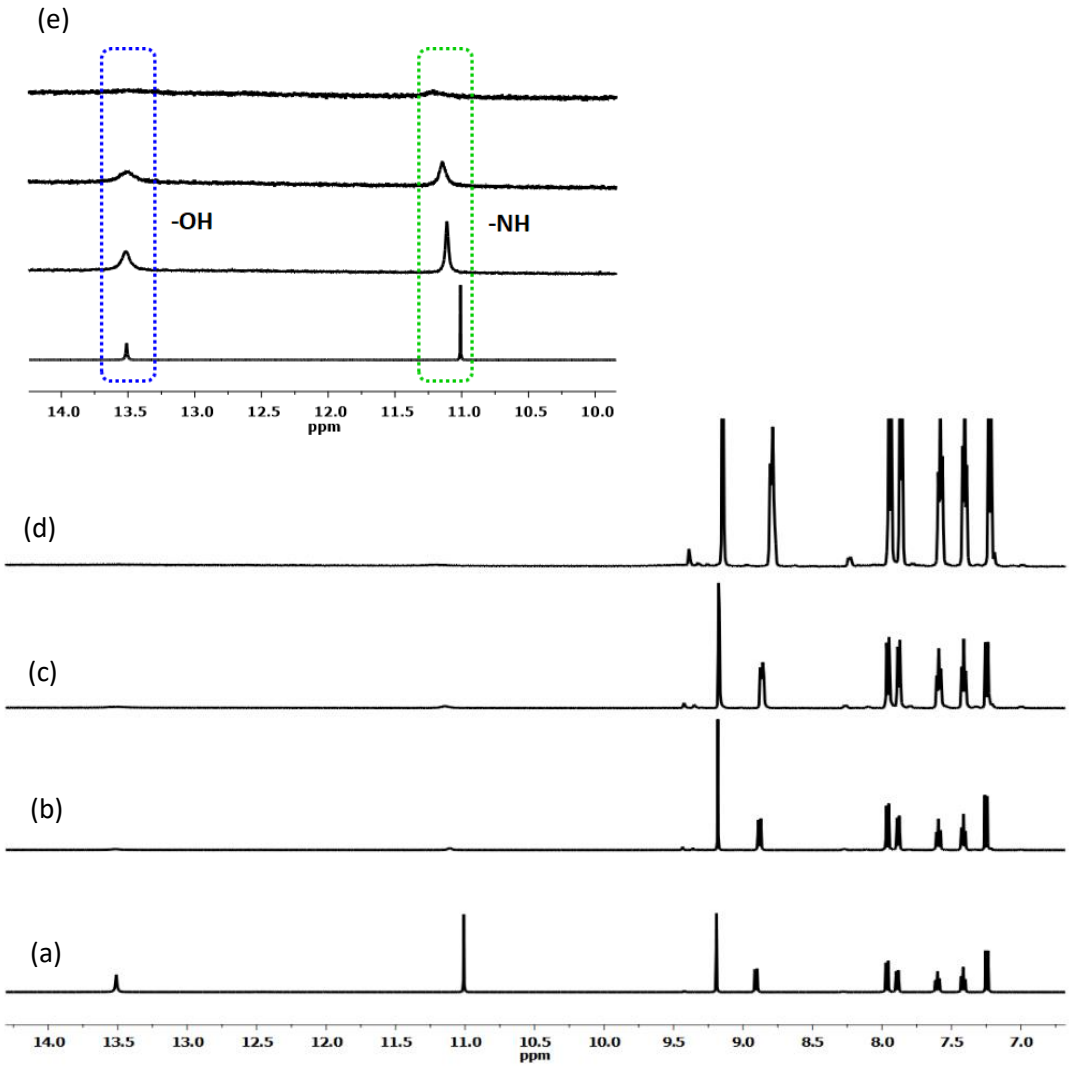

Fig. S17 ^{1}H NMR spectra of NRSB-O in the presence of different concentrations of $AlCl_3$ in DMSO-d_6 and D_2O mixture: (a) NRSB-O only, (b) NRSB-O + Al^{3+} (1 equiv.), (c) NRSB-O + Al^{3+} (3 equiv.), (d) NRSB-O + Al^{3+}(5 equiv.), and (e) zoom view of the spectra between 10 to 14 ppm.

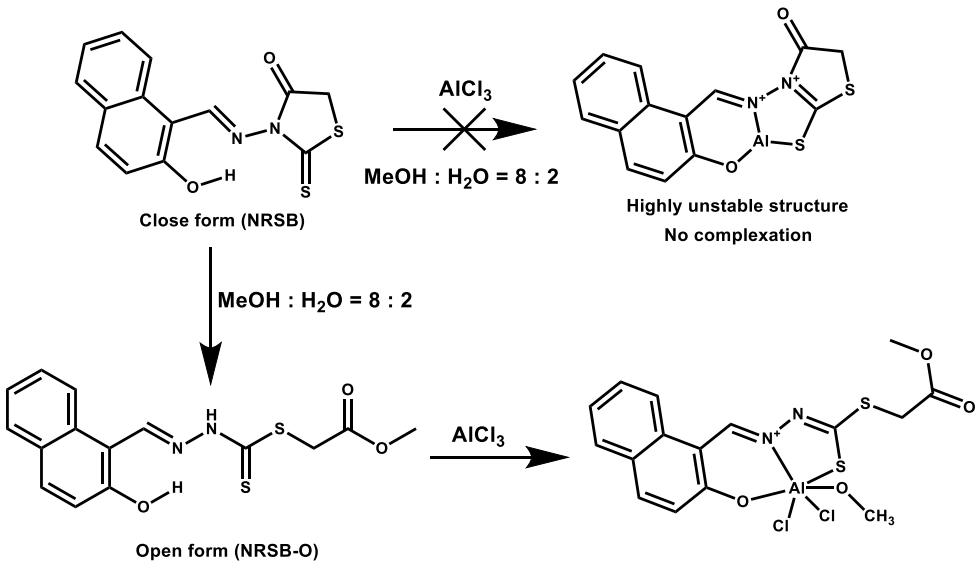

Scheme S1. The proposed complexation of NRSB-O with Al^{3+} in semi-aqueous medium (MeOH : H_2O = 8 : 2).

4. References

1. Q. Deng, Y. Li, J. Wu, Y. Liu, G. Fang, S. Wang and Y. Zhang, *Chem. Commun.*, 2012, **48**, 3009-3011.
2. M. Zhao, Y. Yue, C. Liu, P. Hui, S. He, L. Zhaoa and X. Zeng, *Chem. Commun.*, 2018, **54**, 8339-8342.
3. Z. Wua, X. Fub and Y. Wang, *Sens. Actuators B Chem.,* 2017**, 245**, 406-413.
4. L. Hu, J. Sun, J. Han, Y. Duan and T. Han, *Sens. Actuators B Chem.*, 2017, **239**, 467-473.
5. K. Chung, D. S. Yang, J. Jung, D. Seo, M. S. Kwon and J. Kim, *ACS Appl. Mater. Interfaces*, 2016, **8**, 28124-28129.
6. V. Kumar, A. Kumar, U. Diwan, M. K. Singh and K. K. Upadhyay, *Org. Biomol. Chem.*, 2015, **13**, 8822-8826.
7. Z. Li, X. Liu, W. Zhao, S. Wang, W. Zhou, L. Wei and M. Yu, *Anal. Chem.*, 2014, **86**, 2521-2525.
8. S. Ishihara, N. Iyi, J. Labuta, K. Deguchi, S. Ohki, M. Tansho, T. Shimizu, Y. Yamauchi, P. Sahoo, M. Naito, H. Abe, J. P. Hill and K. Ariga, *ACS Appl. Mater. Interfaces*, 2013, **5**, 5927-5930.
9. X. Zhang and Y. Chen, *Anal. Chim. Acta.*, 2009, **650**, 254-257.
10. U. Saha, M. Dolai and S. Kumar, *New J. Chem.*, 2019, **43**, 8982-8992.
11. T. Qin, B. Liu, Y. Huang, K. Yang, K. Zhu, Z. Luo, C. Pan and L. Wang, *Sens. Actuators B Chem.*, 2018, **277,** 484-491.
12. J. Bourson, J. Pouget and B. Valeur, *J. Phys. Chem.*, 1993, **97**, 4552-4557.
13. J. Wu, W. Liu, J. Ge, H. Zhang and P. Wang, *Chem. Soc. Rev.*, 2011, **40**, 3483.
14. R. Singh, S. Samanta, P. Mullick, A. Ramesh and G. Das, *Anal. Chim. Acta,* 2018, **1025**, 172-180.
15. B. Liu, P. Wang, J. Chai, X. Hu, T. Gao, J. Chao, T. Chen and B. Yang, *Spectrochim. Acta Part A: Mol. Biomol. Spectroscopy*, 2016, **168**, 98-103.